Annales Geophysicae

Dedicated to the memory of Joseph W. Chamberlain, 1928–2004

Nightglow vibrational distributions in the $A^3\Sigma_u^+$ and $A'^3\Delta_u$ states of O_2 derived from astronomical sky spectra

T. G. Slanger[1], P. C. Cosby[1], D. L. Huestis[1], and A. M. Widhalm[2]

[1]Molecular Physics Laboratory, SRI International, 333 Ravenswood Avenue, Menlo Park CA 94025, USA
[2]Department of Physics and Astronomy, University of Southern California, Los Angeles, CA 90089, USA

Abstract. Astronomical sky spectra from the Keck I telescope on Mauna Kea have been used to obtain vibrational distributions in the $O_2(A^3\Sigma_u^+)$ and $O_2(A'^3\Delta_u)$ states from rotationally-resolved Herzberg I and Chamberlain band emissions in the terrestrial nightglow. The $A^3\Sigma_u^+$ distribution is similar to that presented in earlier publications, with the exception that there is significant population in the previously undiscerned v=0 level. The vibrational distributions of the $A'^3\Delta_u$ and $A^3\Sigma_u^+$ states are essentially the same when comparison is made in terms of the level energies. The intensity of Chamberlain band emission at the peak of the distribution is about one-fourth that of the Herzberg I emission, as previously shown, and may be related primarily to radiative efficiency. The peaks in both population distributions are about 0.25 eV below the $O(^3P)+O(^3P)$ dissociation limit. We compare these Herzberg state distributions with that of the $O_2(b^1\Sigma_g^+)$ state, concurring with others that the intense nightglow emission associated with $b^1\Sigma_g^+$(v=0) is a reflection of direct transfer from the Herzberg states. This process takes place following O_2 collisions, with simultaneous production of very high $a^1\Delta_g$ and $b^1\Sigma_g^+$ vibrational levels.

Key words. Atmospheric composition and structure (airglow and aurora; thermosphere composition and structure) – Electromagnetics (miscellaneous)

1 Introduction

The molecular band systems that make up the terrestrial nightglow in the 250–1300 nm spectral region are all, with the exclusion of the OH Meinel bands, products of O-atom recombination. There are five electronically excited states of O_2 that can emit in this region, and each of them is represented by at least one emitting system (Broadfoot and Bellaire, 1999; Chamberlain, 1955; McDade et al., 1986, 1987; Slanger and Copeland, 2003; Slanger and Huestis, 1981). Table 1 lists these transitions, all of which are optically forbidden by one or another selection rule. Because radiative lifetimes are long, collisional deactivation is an important process, and the observed emission intensities reflect not only the production rates but also the loss rates. It is interesting to note that there are only three possible transitions between the upper (A, A', c) and lower (X, a, b) states that are not included in the list – A–a, A–b, and A'–b. The strengths of these transitions are calculated to be non-negligible, (Saxon and Slanger, 1986) and identification could ultimately come from sky spectra. Transitions between Herzberg states, i.e. A–A', A–c, and A'–c are not considered here, as any emission would be well into the infrared and weak.

Atomic recombination starts with the atoms having a potential energy 5.12 eV above the v=0 level of the O_2 ground state. This energy is equivalent to a wavelength of 242 nm, and thus O_2 emission originating with $O(^3P)$ recombination lies at longer wavelengths than this limit. As collisions remove energy, the populations spread out among the various electronic states, and the vibrational distributions reflect the overall dynamics of the interactions.

It is therefore desirable to obtain these distributions as accurately as possible. In particular, there has been considerable work carried out in recent years on determining the loss rate coefficients of the various O_2 electronic states as a function of vibrational level (Copeland et al., 1996; Hwang et al., 1998; Kalogerakis et al., 1999, 2002; Knutsen et al., 1994; Slanger and Copeland, 2003). When combined with the atmospheric vibrational distributions, it will ultimately be possible to characterize the production rates of O_2 vibronic levels, leading to a detailed picture of recombination dynamics.

Of the transitions listed in Table 1, the three for which upper state vibrational distributions have been published are

Correspondence to: T. G. Slanger
(tom.slanger@sri.com)

Table 1. Known O_2 transitions for states below 5.1 eV.

States	Designation	0–0 band origin (cm^{-1})	Observations			
			T	V	M	L
A–X	Herzberg I	35 010	x			x
A'–X	Herzberg III	34 387 (Ω=2)				x
A'–a	Chamberlain	26 346 (Ω=3)	x	x		x
c–X	Herzberg II	32 665	x	x		x
c–a		24 776		x		x
c–b		19 543	x			
b–X	Atmospheric	13 122	x			x
b–a	Noxon	5233	x			x
a–X	IR Atmospheric	7889	x	x	x	x

T   terrestrial
V   Venus
M   Mars
L   laboratory

the Herzberg I and Chamberlain transitions (Slanger and Huestis, 1981; Eastes et al., 1992; Stegman and Murtagh, 1991), and the Atmospheric band system (Slanger et al., 2000a). The Herzberg I system is found to have a peak near v=6, falling sharply to higher v and more gradually to lower v. The highest vibrational level supported by the potential is v=12, of which a few rotational levels have been detected (Huestis et al., 1994; Jenouvrier et al., 1999; Slanger et al., 1996). For the Chamberlain band system there has been only one set of measurements indicating a peak in the distribution near v=7, although no levels below v=5 were reported (Stegman and Murtagh, 1988, 1991). For the Atmospheric band system, there is now known to be a broad and tri-modal distribution, with peaks at v=0, 3/4, and 12 (Slanger et al., 2000a).

A new source of nightglow emission data has recently become available – the astronomical sky spectra from large telescopes (Slanger and Copeland, 2003b; Slanger et al., 1997, 2000a, 2000b, 2003a, 2003b). Those from the Keck I telescope on which we report are obtained at a resolution of ~40 000, and simultaneously cover an extended spectral region. The present work utilizes sky spectra obtained in October and November 1999, with the HIRES (HIgh Resolution Echelle Spectrograph) system on the Keck I telescope, over the 340–500 nm region. This range enables us to obtain distributions for both the $A^3\Sigma_u^+$ and $A'^3\Delta_u$ electronic states, in the Herzberg I and Chamberlain transitions. The Herzberg II transition is discernible in the new spectra but quite weak, and is not included in the analysis. An A–X:c–X system intensity ratio of 4:1 was originally reported from ground-based data (Slanger and Huestis, 1981), but in subsequent analysis of ATLAS/ISO ultraviolet data (Owens et al., 1993; Santoro et al., 1994), where the strongest c–X bands are accessible, the A–X:c–X ratio was estimated to be (10–15):1.

2   Results and discussion

Figure 1 shows an example of the quality of the nightglow spectra obtained from Keck I/HIRES, showing both the Herzberg I 2–6 band and the Chamberlain 6–2 band. As the bands are interleaved, it is essential that we be able to carry out accurate simulations of the line positions and the rotational distribution in a band. The DIATOM program (Huestis, 1994) calculates diatomic band simulations at specified linewidths and temperatures, but requires accurate spectroscopic information, in accordance with the quality of the spectrum being matched. The HIRES spectral resolution in these studies is on the order of 0.01 nm, and thus we need to be able to calculate line positions an order of magnitude more precisely, or 0.001 nm.

We have used the same set of data to improve spectroscopic knowledge of the lower levels of the two transitions under study – the O_2 ground state and the $O_2(a^1\Delta_g)$ state. Previously, information on vibrationally-excited ground state levels has come from observation of the O_2 Schumann-Runge bands in emission, and it has long been realized that intermediate levels, at v=5–8, are not accurately known (Huestis, 1999). For the $O_2(a^1\Delta_g)$ levels, there has been only one set of measurements for levels above v=1, and only for a limited range of rotational levels (Nieh and Valentini, 1987). The upper states of the Herzberg I and Chamberlain transitions, $A^3\Sigma_u^+$ and $A'^3\Delta_u$, are accurately known from absorption measurements (Borrell et al., 1986; Coquart and Ramsay, 1986; Jenouvrier et al., 1999; Kerr and Watson, 1986), although even in this case the Keck data provide new information on the $A'^3\Delta_u(\Omega$=3) component, the upper level of the Chamberlain bands.

We have measured 1280 lines in the Chamberlain bands and a similar number in the Herzberg I bands. It has been demonstrated that the wavelengths are very accurately calibrated by the astronomers with thorium/argon and other lamps, and we are able to check certain dayglow UV lines appearing in the spectra, cf. He (388.9 nm) and Ca^+ (393.4, 396.8 nm), observing that their positions agree with NIST data. As a result, we have precise level positions for $X^3\Sigma_g^-$(v=4–14) and $a^1\Delta_g$(v=1–10) levels, and our previous work on the b–X Atmospheric band system (Slanger, 2000a) provides similar data on $X^3\Sigma_g^-$(v=0–12). Therefore, we are in a position to carry out accurate simulations of the Herzberg I and Chamberlain bands in the Keck spectra.

HIRES is an echelle spectrometer, and the spectra appear in individual orders of the grating, 5–7 nm being covered in a near-UV spectrum. There is generally some overlapping of the orders, which is often not true in the visible and particularly the near-infrared. Observers typically take spectra over a 50-min period, which is adequate to measure star spectra, but not sufficient to measure the weak O_2 features of the UV nightglow. Stegman and Murtagh (1988) have made absolute UV band intensity measurements, and find Herzberg I intensities ranging from 0.5–7 Rayleighs (R), and Chamberlain intensities of 2–5 R. Individual rotational line intensities are then on the order of 100 mR or less. We therefore co-add

spectra; for this study 10–20 spectra were used. We do not limit ourselves to spectra of a single night, and make the implicit assumption that the vibrational and rotational distributions within each O_2 electronic state are invariant.

As yet, we do not have a reliable intensity distribution function over the entire wavelength region investigated. For this reason, the data are analyzed order by order. The requirement is to have two or more bands of either the Herzberg I or Chamberlain system for comparison. For example, in order 101 are found the 3-6 and 5-7 Herzberg I bands, and from their relative intensity we can derive the relative populations in the $A^3\Sigma_u^+$(v=3, 5) levels, given knowledge of the Franck-Condon factors (FCF). In addition, where Herzberg I and Chamberlain bands appear together, as in the spectrum shown in Fig. 1, we can determine the relative intensities of the two systems. In both O_2 systems, the spacing between vibrational levels in the upper states are approximately half that for the lower state levels. Thus, the bands fall in sequences given by v′−v″, (v′+2)–(v″+1), (v′+4)–(v″+2), etc. To the extent allowed by the Franck-Condon factors, we can often find several bands in an order.

The band intensity is proportional to the expression

$$I_{v',v''} = N_{v'} q_{v',v''} \quad \times \quad \nu_{v',v''}^3 \quad \times \quad R_e(r_{v',v''})^2, \qquad (1)$$

where ν is the transition frequency of the band, and R_e is the electronic transition moment, which depends on the internuclear spacing, $r_{v',v''}$. We are seeking the fraction of the emission out of a given v′ represented by a single band. For a sequence of bands as described, there is very little change in the internuclear spacing. For example, for the Chamberlain bands in the sequence beginning with 0–7 and ending with 10-12, the difference in the extreme values of $r_{v',v''}$ is less than 3%, so that under such circumstance R_e can be taken as constant. In any case, the present indication is that transition moments for the Herzberg I system are approximately constant over a relatively large range of internuclear distances (Fateev et al., 1996; Huestis et al., 1994; Merienne et al., 2000; Yoshino et al., 1995). For comparisons within a given order the frequency is also approximately constant, and thus the population ratio between two Herzberg I or Chamberlain bands can be approximated using only Franck-Condon factors and measured intensities. For example, the Herzberg I 0–7 and 6–10 bands are separated by only 0.27 nm, and we can write their population ratio as

$$N_{v=0}/N_{v=6} = (I_{0-7}/I_{6-10}) \times (q_{6-10}/q_{0-7}). \qquad (2)$$

The Franck-Condon factor ratio, calculated from the potentials, is 0.414, while the intensity ratio is found to be 0.51, giving a population ratio of 0.21. Although there is no similar information on the Chamberlain band transition moments, we presume the same arguments hold.

The sequences of bands in an order have the characteristic that there will either be only odd or even emitting levels represented. Thus, the heads of the 3–6 and 5–7 Herzberg I bands are at 354.0 and 355.3 nm, respectively. However, the 4–6 and 4–7 bands are at 345.7 and 363.5 nm, so that one
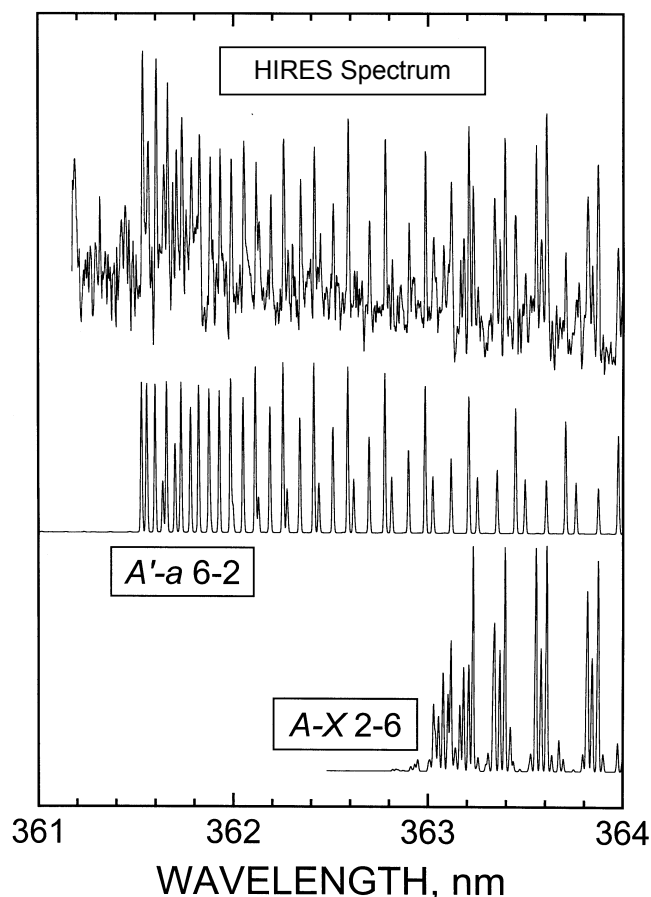

Fig. 1. Keck I/HIRES co-added spectrum of the 361–364 nm region (top). The lower two panels are DIATOM simulations of the $A'^3\Delta_u$–$a^1\Delta_g$ 6–2 band and the $A^3\Sigma_u^+$–$X^3\Sigma_g^-$ 2–6 band.

cannot simultaneously measure $A^3\Sigma_u^+$(v=3, 4, 5) in a single order. We thus adopt the strategy of generating an odd-v and an even-v sequence, then normalizing them so as to give a smooth final distribution. At the shortest wavelengths there are single orders involving both odd and even levels, which is reflected in the plots for the highest vibrational levels. However, there are too few band pairs involving these levels to use them directly in merging the odd and even data.

The data are analyzed by using a least-squares fitting program to construct the observed spectrum from the DIATOM simulations of the component bands in the two O_2 band systems. We include all bands with a reasonable intensity, based on the matrices calculated by Stegman for the two systems (Stegman, 1991). In the simulations the resolution, $\lambda/\Delta\lambda$, is set at 40 000, and the temperature is held fixed at 195 K. The program output is an amplitude coefficient for each band, representing the total band area.

Table 2 presents multiple measured ratios for band pairs in the Herzberg I system. For each pair, the program output intensity is only divided by the Franck-Condon factor. For any pair of upper state levels the population ratio should be the same, regardless of the lower state levels. Thus, the variation
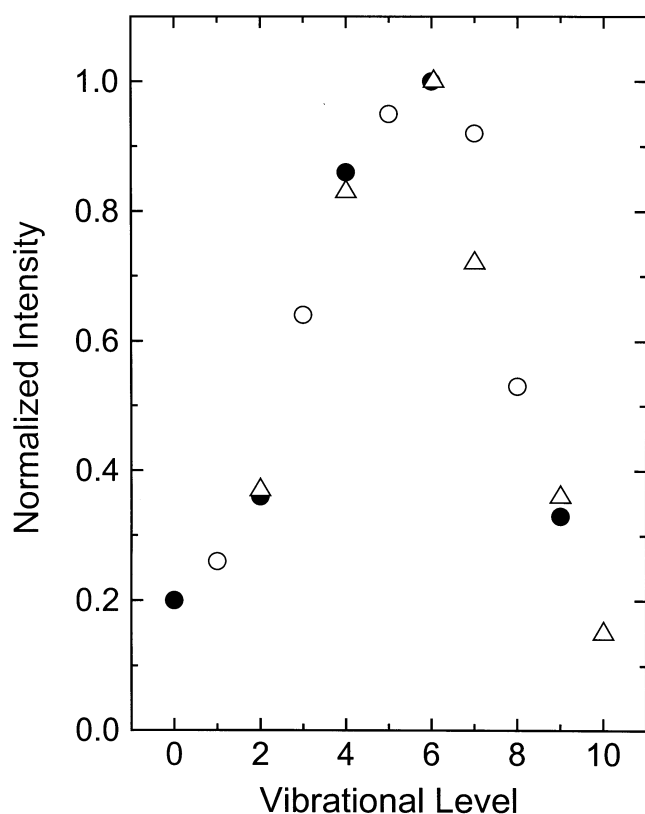
Fig. 2. The $A^3\Sigma_u^+$ vibrational distribution in the nightglow. Open circles – odd-v levels; solid circles – even v-levels; open triangles – data of Stegman and Murtagh (1988). Note that for the high-v levels there is some crossover between the odd and even levels (see text).

Table 2. $O_2(A^3\Sigma_u^+)$ population ratios.

Level pairs	Measured ratios
6/0	5.6, 4.7, 4.5
3/1	2.5, 2.4, 2.4
4/2	2.2, 2.4, 2.6
6/4	1.2, 1.2, 1.1
5/3	1.5, 1.4

in that ratio gives an impression of the error in the procedure. The table shows ratios obtained for band pairs with different lower state levels. For example, the band pairs used to obtain the v(3)/v(1) ratio are 3–5/1–4, 3–6/1–5, and 3–9/1–8. In this instance, the variation for the three examples is less than 5%.

The sets of data are averaged and the vibrational distribution for the $A^3\Sigma_u^+$ state is given in Fig. 2, and shows both the odd-v and even-v sets. It is quite similar to the earliest distribution, which was based on unpublished rotationally unresolved data of Broadfoot (Slanger and Huestis, 1981), to that presented by Stegman and Murtagh where the rotational lines were partially resolved (Stegman and Murtagh, 1991),

Table 3. $O_2(A'^3\Delta_u, \Omega=3)$ population ratios.

Level pairs	Measured ratios
4/2	7.1, 5.5
5/3	2.2, 3.9
6/4	1.8, 2.0
7/5	1.1, 1.3, 1.3
8/6	1.1, 1.0

and to that of the rotationally unresolved data of Eastes, from the S3/4 satellite (Eastes et al., 1992). The new distribution appears to be smooth, without the discontinuity at v=5 (Stegman and Murtagh, 1991). Also shown in Fig. 2 is a partial distribution calculated from absolute intensities (Stegman and Murtagh, 1988) from six Herzberg I bands, normalized to v=6. Except for a discrepancy for v=7, agreement is remarkable. Such comparisons lead us to have confidence in the Chamberlain analysis.

In Table 3 we present a representative data set for Chamberlain band pairs with multiple ratios determined. Here the spread is somewhat greater than for the Herzberg I data, the weaker bands often being weaker than their Herzberg I counterparts. Again, mathematical averages are used when there are multiple determinations.

Figure 3 is a plot of the vibrational distribution in the $A'^3\Delta_u(\Omega=3)$ sub-state, the source of the Chamberlain band emission. As described, the odd and even vibrational level ratios are obtained separately, then combined to give a smooth distribution. Also shown on the plot are the absolute intensity data for four Chamberlain bands measured by Stegman and Murtagh (1988), where we take their intensities and divide them by the fraction of emission from the given v′ represented by the band. The numbers are then normalized to their v=6 peak. The distributions are seen to be quite similar. The $A'^3\Delta_u$ distribution is shifted from that of the $A^3\Sigma_u^+$ state, and the argument has previously been made that such a shift should be expected, and that when plotted on an energy scale, the distributions ought to be similar (Slanger and Huestis, 1981). Lopez-Gonzalez et al. (1992) have modeled a distribution for the $A'^3\Delta_u$ state which is similar to the present one, but with deviations for both high and low vibrational levels.

In Fig. 4 we plot the Herzberg I and Chamberlain distributions as a function of the energy of the levels, and the data show that they are essentially identical; only at the lowest vibrational levels is there significant divergence. As has been previously stated, it appears that the $A^3\Sigma_u^+$ and $A'^3\Delta_u$ states are collisionally coupled for the higher vibrational levels (Slanger and Copeland, 2003), which is now supported by the shape of these distributions. The peak in each case occurs approximately 2000 cm^{-1} below the dissociation limit.

However, the production rate distribution of vibrationally excited levels is more sharply peaked than the population distributions indicate. This is because the collisional loss rates increase with vibrational level; over the $A^3\Sigma_u^+$(v=6–9)
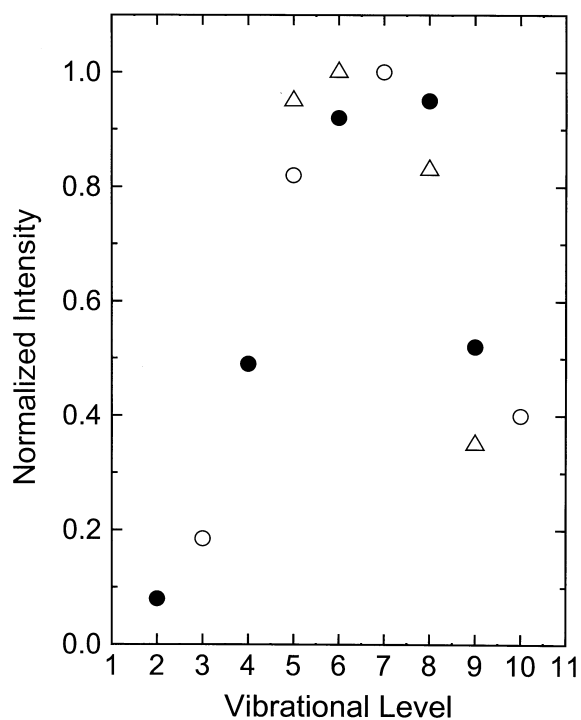
Fig. 3. The $A'^3\Delta_u$ (Ω=3) vibrational distribution in the nightglow. Open circles – odd-v levels; solid circles – even v-levels; open triangles – data of Stegman and Murtagh (1988). Note that for the high-v levels there is some crossover between the odd and even levels (see text).
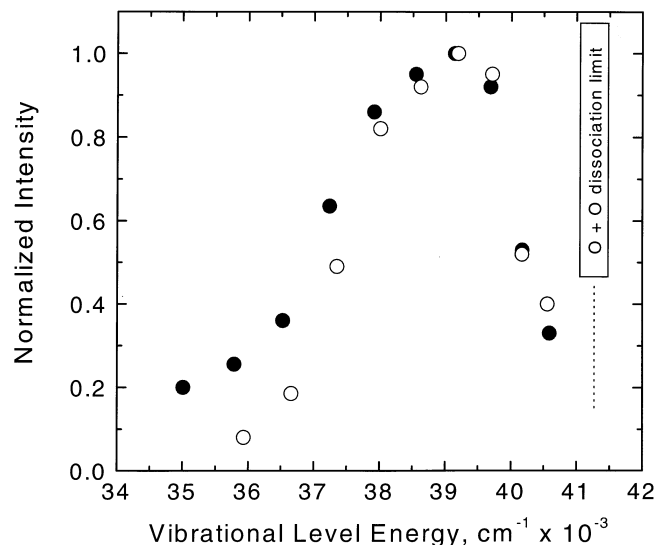

Fig. 4. The $A^3\Sigma_u^+$ (solid circles) and $A'^3\Delta_u$ (open circles) vibrational distributions as a function of the total energy of the levels.

range the O_2 rate coefficient almost doubles and that for N_2 increases by a factor of 6 (Hwang and Copeland, 1997; Copeland and Kalogerakis, 2000). Using the rate coefficients for v=6, 7, 9 and interpolation for v=8, along with an estimated emission altitude of 95 km, we calculate that the production distribution peaks sharply at v=7, 8, with production at v=6 being only half as large, and that at v=9 being 70% as large. The production of the lower levels presumably originates with a relatively inefficient cascading process. These effects will be discussed in a subsequent publication. Such behavior is similar to the situation with OH nightglow emission, where the $H+O_3$ reaction generates OH (v=6–9), and the more intense lower level emissions originate with the high levels, and are essentially amplified by decreasing collisional loss rates (Adler-Golden, 1997).

That the peak of the distribution for production of $A^3\Sigma_u^+$(v) lies at v=7, 8 has at least two possible causes. Work on the $^5\Pi_g$ state of O_2 has shown that it is very important in the recombination process (Amaral et al., 2001; Copeland et al., 2001). On the basis of its degeneracy and the shape of its potential, it seems to be the dominant initial state (Wraight, 1982). Its v=0 level lies at an energy between those of the $A^3\Sigma_u^+$(v=8, 9) levels, and thus the quintet can collisionally feed into v=8 with minimum exchange of energy (Slanger and Copeland, 2003). In addition, there is the situation that if O_2 is the most important collision partner for stabilization of the nascent O_2 molecule, then the ground state fundamental

vibrational quantum, 1556 cm^{-1}, is in near resonance with the $A^3\Sigma_u^+$(v=7) level. Further work is necessary to evaluate these two effects.

It should be kept in mind that the Chamberlain bands represent only a portion of the $A'^3\Delta_u$ population. The Ω=1, 2 sub-levels do not radiate in the $A'^3\Delta_u$–$a^1\Delta_g$ transition, but preferentially radiate in the $A'^3\Delta_u$–$X^3\Sigma_g^-$ Herzberg III bands, which are very weak in the atmosphere or the lab, and would be strongest below 300 nm, and are thus not observable from the ground. How rapidly the three levels collisionally equilibrate is not known.

Noteworthy is the fact that there is substantial population at v=0 in the $A^3\Sigma_u^+$ state distribution, the spectrum in Fig. 5 being the first reported observation of v=0 emission. The DIATOM simulation identifies the lines of the A–X 0–10 band; additional lines belong to the Chamberlain 8–8 band. In a calibrated spectrum obtained with the Keck II+ESI spectrograph system, we have determined an intensity of 2 R for the A–X 0–10 band, from which the emission intensity out of $A^3\Sigma_u^+$(v=0) is calculated to be 14 R for that particular spectrum. Summing the vibrational distribution and relating it to this absolute intensity gives a Herzberg I system intensity of 400 R. Five bands of $A^3\Sigma_u^+$(v'=0) are discernible in the HIRES spectra, for v''=7–11.

In addition to obtaining the vibrational distributions for the $A^3\Sigma_u^+$ and $A'^3\Delta_u$ states, it is possible to compare band intensities of the two transitions in the same order, to obtain a comparison of relative intensities. We earlier reported a ratio of 4:1 for the total intensities in the Herzberg I and Chamberlain systems, respectively (Slanger and Huestis, 1981). Comparison is best done at the peaks of the distributions, and for this purpose we choose to look at the Herzberg I 6–7 band and the Chamberlain 8–2 band. These lie at essentially the same wavelength, and comparison can be made for the same pair of bands measured by Stegman and Murtagh (1988).
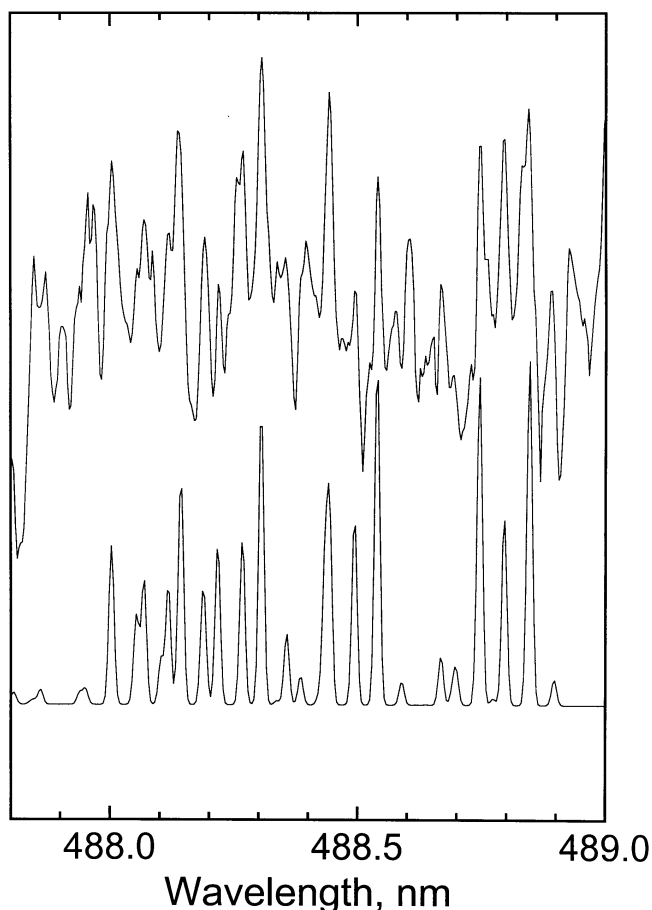
Fig. 5. Keck/HIRES spectrum of the $A^3\Sigma_u^+ - X^3\Sigma_g^-$ 0–10 band (upper) and a DIATOM simulation (lower), additional lines belong to the Chamberlain 8–8 band.
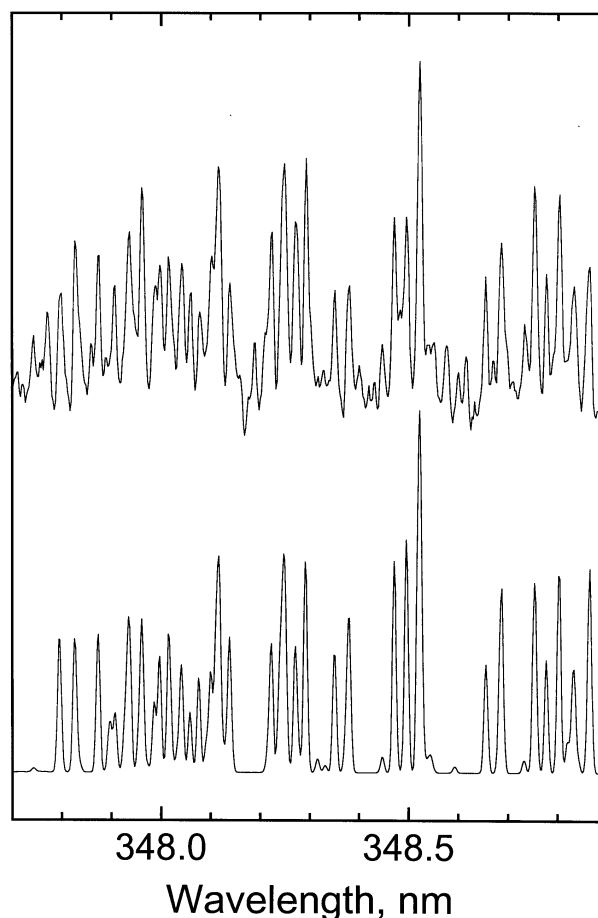
Fig. 6. Comparison of a HIRES spectrum (top) and a DIATOM spectrum (bottom) containing the Herzberg I 6–7 band and the Chamberlain 8–2 band scaled for best fit.

Figure 6 shows the Keck I/HIRES spectrum, and below it a merge of the two O_2 bands scaled to match it. Accounting for the fractions of the level population that the bands represent (the A–X 6–7 band has 9.6% of the emission from $A^3\Sigma_u^+$(v=6) while the A'-a 8–2 band has 27.6% of the emission from $A'^3\Delta_u$(v=8)), we find that the population ratio is 4.1:1 at the peak, where this value would be only slightly modified by summing all the levels. Thus, there is agreement between the present measurements and the earlier results. Stegman and Murtagh (1988) found intensities of 7.29±0.17 R for A–X 6–7 and 5.35±0.24 R for A'-a 8–2, which results in a peak population ratio of 3.95. It should be pointed out that in the spectral region where measurements can be carried out from the ground, the Herzberg I and Chamberlain bands have similar intensities. That the system intensity ratio is four is due to the fact that the Herzberg I bands are much more intense below 300 nm.

It is partially a consequence of differing radiating efficiencies that the Herzberg I emission intensity is four times greater than the Chamberlain intensity. The radiative lifetime of the $A^3\Sigma_u^+$ state is about 160 ms (Huestis et al., 1994), and while there has been no direct determination of

the $A'^3\Delta_u$(Ω=3) radiative lifetime, it is probably 1–2 s. We expect that the removal rate coefficients for the two states are similar at equal energy. In fact, even the $O_2(c^1\Sigma_u^-)$ kinetic data that has been accumulated shows that at equal energies, the $A^3\Sigma_u^+$ and $c^1\Sigma_u^-$ states are removed by O_2 with comparable rate coefficients (Slanger and Copeland, 2003). Thus, it is reasonable to assume that the difference in radiative efficiencies accounts at least in part for the observed emission ratios, and the same reasoning is probably applicable to the c–X emission intensities, where the $c^1\Sigma_u^-$ radiative lifetime is close to 4 s (Huestis et al., 1994).

With knowledge of the $A^3\Sigma_u^+$ and $A'^3\Delta_u$ distributions, it is interesting to compare them to that of the $b^1\Sigma_g^+$ state. The $A^3\Sigma_u^+/A'^3\Delta_u$ populations are strongly peaked at relatively high vibrational levels, but the $b^1\Sigma_g^+$ population appears to collapse down to v=0 (Slanger et al., 2000a). We know that the excited vibrational levels in both states are rapidly relaxed by O_2 collisions (Bloemink et al., 1998; Hwang et al., 1999; Kalogerakis et al., 2002), but for $b^1\Sigma_g^+$(v=0) the relaxation (by N_2) is quite slow (Sander et al., 2003); in the 95 km region, the collisional removal and radiative rates are about the same. For the $A^3\Sigma_u^+$(v=0) level, where the radiative rate

is $6\,s^{-1}$, if collisional removal is entirely by O_2, then the situation would be equivalent if the O_2 rate coefficient had a value of $1\times10^{-12}\,cm^3\,s^{-1}$.

The only literature value for the low-v rate coefficients comes from the work of Kenner and Ogryzlo (1980). They give a value of $(2.9\pm2.0)\times10^{-13}\,cm^3\,s^{-1}$ for the Herzberg I emission seen at 280–400 nm in a discharge flow system, which is primarily from v=1–3. Subsequently, they reported a value of $1.3\times10^{-13}\,cm^3\,s^{-1}$ for the v=2 level (Kenner and Ogryzlo, 1983). Recent investigations indicate that these numbers are probably too small, by at least an order of magnitude (Kirillov, 2002; Slanger and Copeland, 2003). Even so, a figure of $1\times10^{-12}\,cm^3\,s^{-1}$ is a reasonable estimate, thus equating the radiating efficiency for the lowest levels of the $A^3\Sigma_u^+$ and $b^1\Sigma_g^+$ states. Since the fractional emissions out of the v=0 levels of the two states is so dramatically different, we conclude that the behavior of the two states is different in kind, and that the mechanisms of production and loss are not the same.

Such a conclusion is consistent with what we currently believe. Wildt et al. (1991) have shown that when the higher levels of the $A^3\Sigma_u^+$ state are excited, $b^1\Sigma_g^+$(v=0) is promptly formed upon O_2 collision (Wildt et al., 1991), and this observation has been confirmed (Shiau et al., 1998). It has also been shown by Ogryzlo et al. (1984) that in a discharge flow with recombining O-atoms in N_2, $b^1\Sigma_g^+$(v=0) emission is not seen until O_2 is added. Therefore, $O_2(b^1\Sigma_g^+)$ is not produced directly in significant quantities by atom recombination, but requires collisions with O_2; N_2 collisions do not give the same result. It follows that the $b^1\Sigma_g^+$(v=0) seen in the atmosphere from the 95 km region mirrors Herzberg state production, and is not a primary product, as has often been discussed (Bates, 1995; McDade et al., 1986). In particular, its primary source is not cascading within the $b^1\Sigma_g^+$ manifold.

Similarly, for the $A^3\Sigma_u^+$ state there is evidence that cascading is a minor process for the upper vibrational levels investigated. For instance, following v=7 excitation there is relatively little v=6 generated in air (Slanger and Copeland, 2003), and so the atmospheric vibrational distribution peaks at high v near its source, the energy of the recombining atoms. Even in laboratory afterglows in pure O_2 at much higher pressure (McNeal and Durana, 1969), the $A^3\Sigma_u^+$ state vibrational distribution resembles the mesospheric distribution. There is therefore a coherent picture emerging, in which the difference between the $A^3\Sigma_u^+/A'^3\Delta_u$ and $b^1\Sigma_g^+$ distributions is a consequence of the energy transfer process in which the Herzberg state population is converted in one step to $b^1\Sigma_g^+$(v=0). In a sense, this often studied emission is anomalous, and does not represent the $b^1\Sigma_g^+$ state population as such, but is a collector for the Herzberg state population. For observation of processes within the $b^1\Sigma_g^+$ manifold, it is necessary to investigate $b^1\Sigma_g^+$(v>0).

In fact, we see evidence for the analogous situation with $O_2(a^1\Delta_g$, v=0) production (Kalogerakis et al., 2000). It is promptly formed following $A^3\Sigma_u^+$ (v=7) generation, with si-

multaneous production of very high vibrational levels of both the $a^1\Delta_g$ and $b^1\Sigma_g^+$ states, the maximum levels observed ($a^1\Delta_g$(v=19) and $b^1\Sigma_g^+$(v=15)) being resonant with simultaneous $a^1\Delta_g$(v=0) formation. It has also been shown that $a^1\Delta_g$(v=0) production in an $O(^3P)/N_2$ discharge flow system, where $O_2(A–X)$ emission is intense, and requires the addition of O_2 to create the $O_2(a)$(Ali et al., 1986).

In this discussion, we have barely alluded to $O_2(c^1\Sigma_u^-)$, the third of the O_2 Herzberg states. This state is the source of the strong Herzberg II emission in the Venus atmosphere, which is seen in the c–X transition but only from $c^1\Sigma_U^-$(v=0) (Krasnopolsky, 1986). We do not yet carry out the same analysis for this system from Keck data, because the terrestrial bands are quite weak. Stegman and Murtagh (1988) list intensities of 0.26–0.9 R for the three bands they examined. Two of these bands, c–X 8-6 and 7-6, are discernible in the Keck data, and we estimate that the c–X 8–6 band is an order of magnitude weaker than the neighboring A–X 2–5 band, in agreement with the intensities reported by Stegman and Murtagh (1988). We have recently shown that there is another $O_2(c^1\Sigma_u^-)$ transition that is far easier to observe – the c–b bands – and lines of this system are seen throughout the 400–450 nm region (Slanger et al., 2003b).

Curiously, we are not yet in a position to determine a population distribution for the $O_2(c^1\Sigma_u^-)$ state from these bands, because of the nature of the transition. For the Herzberg I and Chamberlain systems, it is possible to say that the radiative transition probabilities out of each vibrational level are approximately the same, and thus that the intensities are only related to production and loss terms (and Franck-Condon factors). For the c–b transition this is not the case – the transition strength is strongly dependent on the energy gap between the $c^1\Sigma_u^-$ state vibrational level and the $1^1\Pi_u$ perturbing state that drives the transition. As a result, we see relatively strong emission from the v=8-11 $c^1\Sigma_u^-$ state levels, but no emission from levels below v=4. That this is not necessarily an indication of a smaller production rate into the low levels is confirmed by noting that neither in the Venus atmosphere, where $c^1\Sigma_u^-$(v=0) emission in the c–X bands is quite intense (Krasnopolsky, 1986), nor in the laboratory, where the same condition can be set up (Lawrence et al., 1977; Slanger, 1978), is there any indication of $c^1\Sigma_u^-$(v=0)-$b^1\Sigma_g^+$(v) emission in the expected 650–750 nm range. Thus, although it is likely that the $c^1\Sigma_u^-$ state population decreases towards low vibrational levels, as seen for the $A^3\Sigma_u^+$ and $A'^3\Delta_u$ states, the observed c–b intensity distribution cannot be interpreted in the same way. Nevertheless, the strongest c–b bands seen in the atmosphere are from the $c^1\Sigma_u^-$(v=9, 10) levels, the energies of which fall near the peaks of the $A^3\Sigma_u^+$ and $A'^3\Delta_u$ distributions shown in Fig. 4. It has previously been argued that the three states are collisionally coupled, and that transfer between them is facile (Slanger and Copeland, 2003). Thus, it is hardly surprising to find the population of each maximizing at comparable energies. As noted above, emission from the $c^1\Sigma_u^-$(v=7, 8) levels in the c–X transition are identifiable in the Keck spectra, but the stronger bands near

the peak of the energy distribution are at shorter wavelengths, and not observable from the ground. We estimate that the c–X and c–b systems have comparable intensity, about 30 R, but the c–b bands are far easier to identify, both because of their much lower spectral line density, giving more photons per line, and because the strongest c–X bands cannot be seen from the ground.

3 Conclusions

The nightglow vibrational distributions of the $O_2 A^3\Sigma_u^+$ and $A'^3\Delta_u$ states have been measured from rotationally-resolved sky spectra obtained with the HIRES echelle spectrograph at the Keck I telescope on Mauna Kea. The $A^3\Sigma_u^+$(v) distribution is very similar to that measured a number of years ago, with the exception that with more complete data, we now find the population in the v=0 level to be substantially larger, being 20% of the peak population at v=5, 6. The $A'^3\Delta_u$ and $A^3\Sigma_u^+$ distributions are almost identical when expressed in terms of the internal energy of the molecule. Both distributions peak at about 2000 cm^{-1} below the dissociation limit, but the more rapid collisional removal with increasing vibrational level at v≥6 in the $A^3\Sigma_u^+$ state implies that most of the atom recombination production starts in the highest levels. We have compared the relative emission intensity ratios at the peak of the $A^3\Sigma_u^+$ and $A'^3\Delta_u$ distributions and find $A^3\Sigma_u^+$ emission to be the more intense by a factor of four, consistent with earlier studies. The $A^3\Sigma_u^+$/$A'^3\Delta_u$ atmospheric distributions contrast strongly with that of the $b^1\Sigma_g^+$ state, and probable reasons are discussed.

References

Adler-Golden, S.: Kinetic Parameters for OH Nightglow Modeling Consistent with Recent Laboratory Measurements, J. Geophys. Res., 102, 19 969–19 976, 1997.

Ali, A. A., Ogryzlo, E. A., Shen, Y. Q., and Wassell, P. T.: The Formation of $O_2(a^1\Delta_g)$ in Homogeneous and Heterogeneous Atom Recombination, Canadian Journal of Physics, 64, 1614–1620, 1986.

Amaral, G. A., Lapcharoensap, W., Copeland, R. A., and Huestis, D. L.: Temperature-Dependent Rates and Branching Ratios for $O_2(^5\Pi_g$, v=0, 1), EOS, Transactions of the American Geophysical Union, 82, F955, 2001.

Bates, D. R.: The Nightglow, in Progress and Problems in Atmospheric Chemistry, edited by Barker, J. R., World Scientific, New Jersey, 420–471, 1995.

Bloemink, H. I., Copeland, R. A., and Slanger, T. G.: Collisional Removal of Vibrationally-Excited $O_2(b^1\Sigma_g^+$, v=1, 2) by O_2, N_2, and CO_2, J. Chem. Phys., 109, 4237–4245, 1998.

Borrell, P. M., Borrell, P., and Ramsay, D. A.: High-Resolution Studies of the Near-Ultraviolet Bands of Oxygen: II: the $A^3\Sigma_u^+$–$X^3\Sigma_g^-$ System, Canadian Journal of Physics, 64, 721–725, 1986.

Broadfoot, A. L. and Bellaire, P. J.: Bridging the gap between ground-based and space-based observations of the night airglow, J. Geophys. Res., 104, 17 127–17 138, 1999.

Chamberlain, J. W.: The ultraviolet airglow spectrum, Astrophysics Journal, 123, 277–286, 1955.

Copeland, R. A. and Kalogerakis, K. S.: The Temperature Dependence of the Collisional Removal of $O_2(A^3\Sigma_u^+$, v=6, 7), EOS, Transactions of the American Geophysical Union, 81, F943, 2000.

Copeland, R. A., Kalogerakis, K. S., Chang, B.-Y., and Huestis, D. L.: Collisional Removal of $O_2(^5\Pi_g)$ at 195 and 150 K, EOS, Transactions of the American Geophysical Union, 82, S283, 2001.

Copeland, R. A., Knutsen, K., Onishi, M. E., and Yalçin, T.: Collisional Removal of $O_2(c^1\Sigma_u^-$, v=9) by O_2, N_2, and He, J. Chem. Phys., 105, 10 349–10 355, 1996.

Coquart, B. and Ramsay, D. A.: High-Resolution Studies of the Near-Ultraviolet Bands of Oxygen: III: the $A'^3\Delta_u$–$X^3\Sigma_g^-$ System, Canadian Journal of Physics, 64, 726–732, 1986.

Eastes, R. W., Huffman, R. E., and LeBlanc, F. J.: NO and O_2 Ultraviolet Nightglow and Spacecraft Glow From the S3–4 Satellite, Planet. Space Sci., 40, 481–493, 1992.

Fateev, A. A., Ivanov, V. S., Pravilov, A. M., and Smirnova, L. G.: Relative Einstein Coefficients and Dipole Moments of the $O_2(A^3\Sigma_u^+$, v′–$X^3\Sigma_g^-$, v″; $c^1\Sigma_u^-$, v′–$X^3\Sigma_g^-$, v″) Transitions Measured in Oxygen Atom Recombination Accompanied by Radiation, Journal of Physics B, 29, 1351–1467, 1996.

Huestis, D. L.: DIATOM Spectral Simulation Computer Program, SRI International, Menlo Park, 1994.

Huestis, D. L.: Current Laboratory Experiments for Planetary Aeronomy, in Atmospheres in the Solar System: Comparative Aeronomy, edited by Mendillo, A., Nagy, A., and Waite, J. H., American Geophysical Union, Washington D.C., 245–258, 2002.

Huestis, D. L., Copeland, R. A., Knutsen, K., Slanger, T. G., Jongma, R. T., Boogaarts, M. G. H., and Meijer, G.: Branch Intensities and Oscillator Strengths for the Herzberg Absorption Systems in Oxygen, Canadian Journal of Physics, 72, 1109–1121, 1994.

Huestis, D. L., Cosby, P. C., Slanger, T. G., and Osterbrock, D. E.: High Vibrational Levels and Potential Energy Curves for the O_2 $a^1\Delta_g$, $b^1\Sigma_g^+$, and $X^3\Sigma_g^-$ States Derived from Atmospheric Nightglow Emissions, in 54th International Symposium on Molecular Spectroscopy, Columbus, OH, 1999.

Hwang, E. S., Bergman, A., Copeland, R. A., and Slanger, T. G.: Temperature Dependence of the Collisional Removal of $O_2(b^1\Sigma_g^+$, v=1 and 2) at 110–260 K, and Atmospheric Applications, J. Chem. Phys., 110, 18–24, 1999.

Hwang, E. S. and Copeland, R. A.: Temperature Dependence of the Collisional Removal of $O_2(A^3\Sigma_u^+$, v=9) with O_2 and N_2, Geophys. Res. Lett., 24, 643–646, 1997.

Hwang, E. S., Copeland, R. A., Robertson, R. M., and Slanger, T. G.: Collisional Removal of $O_2(a^1\Delta_g)$ v=1, 2 and Detection of $O_2(a^1\Delta_g)$ and $O_2(b^1\Sigma_g^+)$ from Photodissociation of Ozone at 310–340 nm, EOS, Transactions of the American Geophysical Union, 79, F85, 1998.

Jenouvrier, A., Merienne, M.-F., Coquart, B., Carleer, M., Fally, S., Vandaele, A. C., Hermans, C., and Colin, R.: Fourier transform spectroscopy of the O_2 Herzberg bands, I. Rotational analysis, Journal of Molecular Spectroscopy, 198, 136–162, 1999.

Kalogerakis, K. S., Copeland, R. A., and Slanger, T. G.: Collisional Removal of $O_2(b^1\Sigma_g^+$, v=2, 3), J. Chem. Phys., 116, 4877–4885, 2002.

Kalogerakis, K. S., Slanger, T. G., and Copeland, R. A.: Temperature dependence of the collisional removal rate constants for $O_2(b$, v=2, 3), EOS, Transactions of the American Geophysical Union, 81, S332, 1999.

Kalogerakis, K. S., Totth, A., Cosby, P. C., Slanger, T. G., and Copeland, R. A.: Laboratory Studies of the Production of Highly Vibrationally Excited $O_2(a^1\Delta_g$ and $b^1\Sigma_g^+)$ from $O_2(A^3\Sigma_u^+)$ Relaxation, EOS, Transactions of the American Geophysical Union, 81, F944, 2000.

Kenner, R. D. and Ogryzlo, E. A.: Deactivation of $O_2(A^3\Sigma_u^+)$ by O_2, O, and Ar, International Journal of Chemical Kinetics, 12, 501–508, 1980.

Kenner, R. D. and Ogryzlo, E. A.: Quenching of $O_2(c^1\Sigma_u^-)$ v=0 by $O(^3P)$, $O_2(a^1\Delta_g)$, and Other Gases, Canadian Journal of Chemistry, 61, 921–926, 1983.

Kerr, C. M. L. and Watson, J. K. G.: Rotational Line Strengths in $^3\Delta$–$^3\Sigma$ Electronic Transitions, The Herzberg III System of Molecular Oxygen, Can. J. Phys., 64, 36–44, 1986.

Kirillov, A.: Calculation of rate coefficients of intramolecular and intermolecular electron energy transfer processes, II Molecular oxygen, in Committee on Space Research (COSPAR), Houston, TX, 2002.

Knutsen, K., Dyer, M. J., and Copeland, R. A.: Laser Double-Resonance Study of the Collisional Removal of O_2 ($A^3\Sigma_u^+$, v=6, 7, 9) with O_2, N_2, CO_2, Ar and He, J. Chem. Phys., 101, 7415–7422, 1994.

Krasnopolsky, V. A.: Oxygen Emissions in the Night Airglow of the Earth, Venus and Mars, Planet. Space Sci., 34, 511–518, 1986.

Lawrence, G. M., Barth, C. A., and Argabright, V.: Excitation of the Venus Night Airglow, Science, 195, 573, 1977.

López-González, M. J., López-Moreno, J. J., and Rodrigo, R.: Altitude and Vibrational Distribution of the O_2 Ultraviolet Nightglow Emissions, Planet. Space Sci., 40, 913–928, 1992.

McDade, I. C., Llewellyn, E. J., Greer, R. G. H., and Murtagh, D. P.: ETON 6: rocket measurement of the O_2 Infrared Atmospheric (0–0) band in the nightglow, Planet. Space Sci., 35, 1541–1552, 1987.

McDade, I. C., Murtagh, D. P., Greer, R. G. H., Dickinson, P. H. G., Witt, G., Stegman, J., Llewellyn, E. J., Thomas, L., and Jenkins, D. B.: ETON 2: Quenching Parameters for the Proposed Precursors of $O_2(b^1\Sigma_g^+)$ and $O(^1S)$ in the Terrestrial Nightglow, Planet. Space Sci., 34, 789–800, 1986.

McNeal, R. J. and Durana, S. C.: Absolute Chemiluminescent Reaction Rates for Emission of the O_2 Herzberg Bands in Oxygen and Oxygen-Inert-Gas Afterglows, J. Chem. Phys., 51, 2955–2960, 1969.

Merienne, M. F., Jenouvrier, A., Coquart, B., Carleer, M., Fally, S., Colin, R., Vandaele, A. C., and Hermans, C.: Fourier transform spectroscopy of the O_2 Herzberg bands, II. Band oscillator strengths and transition moments, Journal of Molecular Spectroscopy, 202, 171–193, 2000.

Nieh, J.-C. and Valentini, J. J.: Molecular Potentials from CARS Photofragment Spectroscopy: Spectroscopic Constants and Potential Energy Curve for $O_2(a^1\Delta_g)$, J. Phys. Chem., 91, 1370–1374, 1987.

Ogryzlo, E. A., Shen, Y. Q., and Wassell, P. T.: The Yield of $O_2(b^1\Sigma_g^+)$ in Oxygen Atom Recombination, Journal of Photochemistry, 25, 389–398, 1984.

Owens, J. K., Torr, D. G., Torr, M. R., Chang, T., Fennelly, J. A., Richards, P. G., Morgan, M. F., Baldridge, T. W., Fellows, C. W., Dougani, H., Swift, W., Tejada, A., Orme, T., Germany, G. A., and Yung, S.: Mesospheric nightglow spectral survey taken by the ISO Spectral Spatial Imager on Atlas 1, Geophys. Res. Lett., 20, 515–518, 1993.

Sander, S. P., Friedl, R. R., Golden, D. M., Kurylo, M. J., Huie, R. E., Orkin, V. L., Moortgat, G. K., Ravishankara, A. R., Kolb, C. E., Molina, M. J., and Finlayson-Pitts, B. J.: Chemical Kinetics and Photochemical Data for Use in Stratospheric Modeling, Evaluation Number 14, National Aeronautics and Space Administration, Jet Propulsion Laboratory, 1, 8, 2003.

Santoro, A. L., Huestis, D. L., and Slanger, T. G.: Spectral Analysis of Atlas I/ISO O_2 Ultraviolet Nightglow Data, and Comparison with Laboratory Afterglows, EOS, Transactions of the American Geophysical Union, 75, F496, 1994.

Saxon, R. P. and Slanger, T. G.: Molecular Oxygen Absorption Continua at 195–300 nm and O_2 Radiative Lifetimes, J. Geophys. Res., 91, 9877–9879, 1986.

Shiau, T. P., Hwang, E. S., Buijsse, B., and Copeland, R. A.: Vibrational-level-dependent Yields of $O_2(b^1\Sigma_g^+$, v=0) Following Collisional Removal of $O_2(A^3\Sigma_u^+$, v), Chem. Phys. Letters 282, 369–374 (1998).

Slanger, T. G.: Generation of $O_2(c^1\Sigma_u^-, C'^3\Delta_u, A^3\Sigma_u^+)$ from Oxygen Atom Recombination, J. Chem. Phys., 69, 4779–4791, 1978.

Slanger, T. G. and Copeland, R. A.: Energetic Oxygen in the Upper Atmosphere and the Laboratory, Chemical Reviews, 103, (12), 4731–4765, 2003.

Slanger, T. G., Cosby, P. C., and Huestis, D. L.: Ground-based observation of high-altitude high-temperature emission in the O_2 Atmospheric band nightglow, J. Geophys. Res., 108, (A7), doi:10.1029/2003JA009885, 2003a.

Slanger, T. G., Cosby, P. C., and Huestis, D. L.: A new O_2 band system: The $c^1\Sigma_u^- - b^1\Sigma_g^+$ transition in the terrestrial nightglow, J. Geophys. Res., 108, (A2), 1089, 2003b.

Slanger, T. G., Cosby, P. C., Huestis, D. L., and Osterbrock, D. E.: Vibrational Level Distribution of $O_2(b^1\Sigma_g^+$, v=0–15) in the Mesosphere and Lower Thermosphere Region, J. Geophys. Res., 105, 20 557–20 564, 2000a.

Slanger, T. G. and Huestis, D. L.: $O_2(c^1\Sigma_u^- - X^3\Sigma_g^-)$ Emission in the Terrestrial Nightglow, J. Geophys. Res., 86, 3551–3554, 1981.

Slanger, T. G., Huestis, D. L., Cosby, P. C., and Osterbrock, D. E.: Accurate Atomic Line Wavelengths from Astronomical Sky Spectra, J. Chem. Phys., 113, 8514–8520, 2000b.

Slanger, T. G., Huestis, D. L., Osterbrock, D. E., and Fulbright, J. P.: The Isotopic Oxygen Nightglow as Viewed From Mauna Kea, Science, 277, 1485–1488, 1997.

Slanger, T. G., Huestis, D. L., Cosby, P. C., Naus, H., and Meijer, G.: O_2 Photoabsorption in the 40 950–41 300 cm^{-1} Region: New Herzberg Bands, New Absorption Lines, and Improved Spectroscopic Data, J. Chem. Phys., 105, 9393–9402, 1996.

Smith, I. W. M.: The Role of Electronically Excited States in Recombination Reactions, International Journal of Chemical Kinetics, 16, 423–443, 1984.

Stegman, J.: Spectroscopic and Kinetic Studies of Atmospheric Oxygen Emissions, Ph. D. thesis, Stockholm University, Stockholm, 40–42, 1991.

Stegman, J. and Murtagh, D. P.: High Resolution Spectroscopy of Oxygen U.V. Airglow, Planet. Space Sci., 36, 927–934, 1988.

Stegman, J. and Murtagh, D. P.: The Molecular Oxygen Band Systems in the U.V. Nightglow: Measured and Modelled, Planet. Space Sci., 39, 595–609, 1991.

Wildt, J., Bednarek, G., Fink, E. H., and Wayne, R. P.: Laser Excitation of the $A^3\Sigma_u^+$, $A'^3\Delta_u$, and $c^1\Sigma_u^-$ States for Molecular Oxygen, Chemical Physics, 156, 497–508, 1991.

Wraight, P. C.: Associations of Atomic Oxygen and Airglow Excitation Mechanisms, Planet. Space Sci., 30, 251–259, 1982.

Yoshino, K., Esmond, J. R., Murray, J. E., Parkinson, W. H., Thorne, A. P., Learner, R. C. M., and Cox, G.: Band Oscillator Strengths of the Herzberg I Bands of O_2, J. Chem. Phys., 103, 1243–1249, 1995.